NIH Public Access
Author Manuscript
*Inorganica Chim Acta*. Author manuscript; available in PMC 2015 March 01.

Published in final edited form as:
*Inorganica Chim Acta*. 2014 March 1; 412: 94–103. doi:10.1016/j.ica.2013.12.006.

# Synthesis and Characterization of Two Cyanoxime Ligands, Their Precursors, and Light Insensitive Antimicrobial Silver(I) Cyanoximates.

**Courtney N. Riddles**[1], **Mark Whited**[1], **Shalaka R. Lotlikar**[2], **Korey Still**[2], **Marianna Patrauchan**[2], **Svitlana Silchenko**[3], and **Nikolay Gerasimchuk**[1,*]

[1]Department of Chemistry, Temple Hall 456, Missouri State University, Springfield, MO 65897

[2]Department of Microbiology and Molecular Genetics, 307 Life Sciences East, Oklahoma State University, Stillwater, OK 74078.

[3]Absorbtion Systems, Inc. 440 Creamy Way, S.300, Exton, PA 19341.

## Abstract

High-yield syntheses of N-piperidine-cyanacetamide (**1**), N-morpholyl-cyanacetamide (**4**) and their oxime derivatives N-piperidine-2-cyano-2-oximino-acetamide (HPiPCO, **2**) and N-morpholyc-2-cyano-2-oximino-acetamide (HMCO, **5**) were developed using two-step preparations. At first, the reactions of neat cyanoacetic acid esters and the respective cyclic secondary amines such as piperideine and morpholine afforded pure cyanacetamides, which were converted into cyanoximes at room temperature using the nitrosation reaction with gaseous $CH_3ONO$. The synthesized compounds were investigated by means of IR, $^1H$, $^{13}C$ and UV-visible spectroscopy. Crystal structures of two starting substituted cyan-acetamides and two target cyanoximes were determined. Silver(I) complexes of AgL composition (L = PipCO, **3**; MCO, **6**) were prepared in high yield. Both metal complexes are thermally stable above 100°C, and remarkably stable to high intensity visible light. The stability of dried AgL compounds towards short wavelength UV-radiation (a frequently used germicidal light) was examined using diffusion reflectance spectroscopy. Both complexes demonstrate slow photoreduction within ~3 hrs, observable as a gradual color change and darkening due to the formation of fine (nano-scale)

© 2013 Elsevier B.V. All rights reserved.

*Corresponding authors: NNGerasimchuk@MissouriState.edu; phone: 1-417-836-5165.

**Publisher's Disclaimer:** This is a PDF file of an unedited manuscript that has been accepted for publication. As a service to our customers we are providing this early version of the manuscript. The manuscript will undergo copyediting, typesetting, and review of the resulting proof before it is published in its final citable form. Please note that during the production process errors may be discovered which could affect the content, and all legal disclaimers that apply to the journal pertain.

Pages of ***Electronic Supporting Information*** available: experimental setup for generation of gaseous $CH_3ONO$ (*ESI 1*); details of preparation of samples of solid Ag(I) cyanoximates for photophysical studies (*ESI 2*); hardware for UV-light irradiation experiments and recording of reflectance spectra (*ESI 3*); content of flowable light-curable composites for mixing with solid Ag(I) cyanoximates (*ESI 4*); experimental details of making polymeric composites (*ESI 5*); 96-wells plate and commercial light source (used in dentistry) which were employed in fabrication of samples for antimicrobial studies (*ESI 6*); actual photographs of 96-wells plates with solidified acrylate composite containing Ag(I) cyanoximates (*ESI 7*); crystal data for precursors **1** and **4** (*ESI 8*); selected bond lengths and valence angles in the structures of precursors for cyanoximes – acetamides **1** and **4** (*ESI 9*); $^{13}C\{^1H\}$ NMR spectra of precursors **1** and **4** (*ESI 10,11*); checkCIF reports for structures of precursors **1** and **4** (*ESI 12,13*); packing diagram and H-bonding pattern in the structure of the cyanoxime **5** (*ESI 14*); packing diagram and H-bonding pattern in the structure of the cyanoxime **2** (*ESI 15*); planes in the molecule of **5** (*ESI 16*); planar fragments in the structure of **2** (*ESI 17,18*); table of H-bonding in the structures of **2** and **5** (*ESI 19*); checkCIF report for the crystal structure of **2** (*ESI 20*); checkCIF report for the crystal structure of **5** (*ESI 21*); UV-visible spectra of aqueous solutions of protonated and deprotonated **5** (*ESI 22*); solvatochromic series for the anion of cyanoxime **5** (*ESI 23*); solvatochromic series for the anion of cyanoxime **2** (*ESI 24*); NMR data for **5** (*ESI 25*); NMR data for **2** (*ESI 26,27*); reflectance spectra of standard MgO and light-sensitive AgCl and $AgNO_3$ (*ESI 28-30*); light sources used for curing of flowable acrylate composites (*ESI 31*).

NIH-PA Author Manuscript
NIH-PA Author Manuscript
NIH-PA Author Manuscript

NIH-PA Author Manuscript

NIH-PA Author Manuscript

NIH-PA Author Manuscript

particles of metallic silver. The complex Ag(MCO), **6**, is about 2.6 times less stable towards UV-radiation than its more lypophyllic analog Ag(PipCO), **3**. Antimicrobial and biofilm growth inhibition properties of the prepared solid acrylate-based polymeric composites containing embedded silver(I) cyanoximates were investigated using three human pathogens: *P. aeruginosa* PAO1 (wound isolate), *S. aureus* NRS70 (methicillin resistant respiratory isolate), and *S. mutans* UA159 (cariogenic dental isolate). Studies showed that both **3** and **6** compounds completely abolished the growth of PAO1 at 0.5 weight % concentration, and the growth of UA159 and NRS70 at 1% concentration. Moreover, data demonstrates that complexes **3** and **6** also inhibit both planktonic and biofilm growth of Gram-positive and Gram-negative bacterial pathogens. The demonstrated thermal stability and pronounced antimicrobial activity of both silver(I) cyanoximates indicates the strong potential for the studied complexes to be used as light insensitive antimicrobial additives to light-curable adhesives that set indwelling devices in place.

### Keywords

cyanoximes; UV-visible spectra; X-ray analysis; silver(I) complexes; antimicrobial activity; biofilm inhibition

## Introduction

Bacterial biofilms are structured communities of bacteria that are commonly embedded in a self-produced matrix, mostly consisting of polysaccharides, proteins and DNA. Bacterial biofilms cause severe chronic infections that are increasingly difficult to treat due to the unique physiology of biofilm cells, which have a high tolerance for antibiotics and disinfecting chemicals as well as resistance to the host defensive processes. The underlying mechanisms include gradients of nutrients and oxygen, decreased metabolic activity and growth rates, adaptability associated with elevated levels of mutations, horizontal gene transfer and quorum-sensing-regulated mechanisms, as well as a combination of multiple conventional mechanisms of resistance such as energy-dependent efflux, chromosomally encoded β-lactamases, low outer membrane permeability, and modifications in the target molecules. Currently, early aggressive eradication antibiotic therapy is used to prevent biofilm infections, and long-term suppressive antibiotic therapy is used to treat chronic biofilm infections [1]. New promising strategies are being developed that use enzymes, e.g. DNase and alginate lyase, to dissolve the major component of the biofilm matrix [2] or quorum-sensing inhibitors to increase the biofilm's susceptibility to antibiotics [3]. However, the remaining challenges include continuously increasing resistance to antibiotics, which requires the development of new types of antimicrobials and targeted delivery of the drugs.

Bacterial biofilms are particularly problematic in device-associated infections and typically include multiple diverse species. The main organism infecting internal devices is *Staphylococcus aureus*, and the secondary pathogens include *Pseudomonas aeruginosa* and *Streptococcus spp.* [4]. *Streptococcus mutans* is also the most common causative agent of dental carries [5]. Because biofilms resist antibiotics, they introduce one of the most challenging paradoxes in modern medicine: devices such as pacemakers, defibrillators and prosthetic cardiac valves save lives, but they cause infections in about 4 percent of the estimated one million patients receiving implants each year in the United States. The only available and efficient treatment of these infections is surgery to remove the contaminated device and implant a new one. This adds up to thousands of surgeries and more than $1 billion in health care costs every year [6].

The development of new infection-preventing strategies and antibacterial agents in particular are a critical priority as artificial implant therapy rapidly increases in use. One of

NIH-PA Author Manuscript

NIH-PA Author Manuscript

NIH-PA Author Manuscript

the interesting options is an introduction of the non-antibiotic antimicrobial substance, for example, into the glue used during the introduction of indwelling medical devices, or provide the surface treatment of such devices to prevent pathogenic cell adhesion and biofilm formation. Therefore, the search for new implant materials that would prevent post-surgical infections requires new knowledge about chemical compounds that would inhibit bacterial growth but, at the same time, would not be toxic to human tissues. In summary, there is a critical need in non-antibiotic compounds that satisfies specific needs to be water insoluble, light- and chemically stable, and yet can survive sterilization at 100°C without decomposition. Pure organic compounds can't meet these criteria, but coordination-polymeric metal complexes can. Therefore, it is important to identify and study new metal-based compounds that will meet these demands.

Silver has long been known for its antibacterial properties. In fact, long ago, people used silver-lined containers to safely store their water. Even today, silver is used in burn therapy, adhesive bandages, and numerous other preventative methods [7]. One of the applications of silver and its compounds is the reduction of postoperative infections caused by implants. Thus, silver compounds were loaded into some implant materials such as bioglass [8] and bone cement [9]. It is reported that the incorporation of silver into implants is a most promising method in reducing the infection rate, while exhibiting low toxicity towards cells and tissues [10]. Silver-incorporating biomaterials, therefore, have tremendous potential for advancing the safety of internal implant therapies in the health care industry [11-13]. However, there were no silver(I) compounds that combine light and thermal stability, chemical inertness, water insolubility and show antimicrobial activity. Thus, the greatest challenge with common silver(I) inorganic compounds known for their antimicrobial properties is a reduction back to elemental silver upon exposure to light and heat [14]. Nevertheless, there is one particular class of low molecular weight organic compounds that can act as ligands for binding silver(I) cations and will form complexes that satisfy the specific requirements outlined above. These compounds are oximes, which represent versatile organic molecules that were extensively used as excellent ligands in analytical [15], inorganic [16-20] and bioinorganic chemistry [21-23]. Cyanoximes – compounds with the general formula HON=C(CN)-R (R = electron withdrawing group) – represent a new, special class of biologically active molecules [24], and their chemistry and biomedical applications have been intensively developed in the last two decades [25]. These molecules also act as excellent ligands capable of binding to different metal ions [26-28]. The presence of the CN-group significantly increases their acidity and makes them better ligands for binding metal ions as compared to conventional monoximes. There are 37 currently known and studied in various laboratories around the world cyanoximes [44]. Earlier data showed no intrinsic *in vitro* cytotoxicity of free organic cyanoximes [29-31]. We recently discovered that some silver(I) cyanoximates are *insoluble in water*, represent *thermally and chemically stable* compounds [32-35], and also exhibit *significant antimicrobial activity* [36]. Since silver(I) cyanoximates possess these properties valuable for biomedical application, their thorough investigation is warranted. With the exception of several publications [37-39], there were no systematic studies regarding light-stable silver(I) antimicrobial compounds targeting specific infections, and no oxime-based compounds were tested on that matter at all.

In this study we report preparation and crystal data for two new shown below cyanoximes, 2-cyano-2-isonitroso-N-piperidynylacetamide (further HPiPCO, compound **2**) and 2-cyano-2-isonitroso-N-morpholylacetamide (later HMCO, compound **5**), and their precursors. Also, two new silver(I) complexes with both cyanoximes were synthesized and characterized using a variety of techniques including photo-stability studies towards visible and UV-light. The cyanoximes **2** and **5** have markedly different water solubility and

NIH-PA Author Manuscript

NIH-PA Author Manuscript

NIH-PA Author Manuscript

hydrophobicity, which makes their comparative studies and investigations of their metal complexes especially interesting.

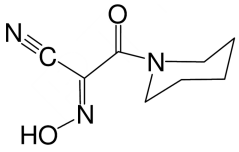

HPiPCO, **2**

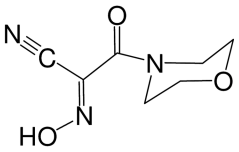

HMCO, **5**

## Experimental Part

Scheme 1 contains the synthetic route to the cyanoximes used in this study, as well as the adopted numbering format for all obtained compounds in this paper.

### Chemicals and Instrumentation

The ethylcyanoacetate, piperidine, morpholine, $NaNO_2$, 1-propanol, and acids were all reagent grade (ALDRICH) and used without further purification. The TLC for the ligand and its precursor were carried out on silica-coated glass plates (Merck), containing a 256 nm fluorescent indicator. Elemental analyses on C,H,N content were performed at the Atlantic Microlab (Norcross, GA). Melting points were measured on a Digimelt apparatus without correction. Ionization constants for two new cyanoximes **2** and **5** were determined using a Sirius Analytical Instruments automated titration station (Sussex, UK) equipped with a temperature-controlled bath. The titration was performed at 23°C in the isopropyl alcohol (later ISA) - water mixture for the HMCO (**5**), and in ISA-MeOH mixtures for the HPiPCO (**2**), due to its insolubility in water. The weighed amount of HMCO, **5**, (2.29 mg) was placed into a titration vial. Sixteen milliliters of ISA water was delivered automatically to the vial. The pH of the solution was adjusted to 2 by adding 0.5 M of HCl automatically. The titration with 0.5M of KOH was performed automatically until a pH value of 11 was reached. To perform the second and third titrations, an additional volume of ISA water (1 mL and 1 mL) was delivered automatically to the titration vial, respectively. The datasets for the three titrations were combined in the RefinementPro program to create a Multiset for a $pK_a$ calculation. The titration was performed at 23°C in the MeOH/ISA water mixture. The weighed amount of HPiPCO, **2**, (3.53 mg) was placed into a titration vial. 7 mL of 80% aqueous MeOH followed by eight milliliters of ISA water was delivered automatically to the vial. The pH of the solution was adjusted to 3 by adding 0.5M of HCl automatically. The titration with 0.5M of KOH was performed automatically until a pH value of 11 was reached. To perform the second and third titrations, an additional volume of ISA water (2 mL and 1 mL) was delivered automatically to the titration vial, respectively. The datasets for the three titrations were combined and extrapolated to zero MeOH concentration. The aqueous pKa was calculated with Yasuda-Shedlovsky extrapolation in the RefinementPro software.

### Spectroscopy

Synthesized organic compounds **1**, **2**, **4** and **5** were characterized by $^{1}H$, $^{13}C$ NMR spectroscopy (solutions in dmso-$d_6$; TMS was an internal standard; Varian INova 400 MHz spectrometer; T = +25°C). The UV-visible spectra of the cyanoximes **2** and **5** and their anions were recorded at room temperature (293 K) using an HP 8354 spectrophotometer in the range of 200 – 1100 nm, in 1 mm and 10 mm quartz cuvettes (Starna, Inc.). Infrared spectra were recorded in the range of 500–4000 $cm^{-1}$, in KBr pellets (for **1**, **2**, **4** and **5**) using the FT-IR Bruker Vertex 70, or FT-ATR Bruker spectrophotometer for **3** and **6**.

NIH-PA Author Manuscript

NIH-PA Author Manuscript

NIH-PA Author Manuscript

## X-Ray Crystallography

Crystal structures were determined for all four presented in this work organic compounds: substituted cyan-acetamide precursors **1** and **2**, and respective cyanoximes **2** and **5**. Suitable single crystals of these compounds were mounted on a thin galls fiber attached to the copper-pin positioned on the goniometer head of the Bruker APEX 2 diffractometer, equipped with a SMART CCD area detector. Data sets were measured at 120 K. The intensity data were collected in ω scan mode using the Mo tube (Kα radiation; λ = 0.71073 Å) with a highly oriented graphite monochromator. Intensities were integrated from 4 series of 364 exposures, each covering 0.5$^{o}$ in ω at 20 seconds of acquisition time, with the total data set being a sphere [40]. The space group determination was done with the aid of XPREP software [40]. The absorption correction was performed using the SADABS program that was included in the Bruker AXS software package [41]. All structures were solved by direct methods and refined by least squares on weighted $F^2$ values for all reflections using the SHELXTL program. Drawing of crystal structures and packing diagrams was done using the ORTEP [42] and Mercury software packages [43]. All four crystal structures have been deposited into the CCDC under the following numbers: **1** – 956130, **2** – 956128; **4** – 956129; **5** – 956127. The PLATON checkCIF reports are shown in the *Electronic Supporting Information* section.

## Synthesis

***Preparation of N-substituted cyanacetamides* 1 *and* 4 *– precursors to the cyanoximes—***Neat ethylcyanoacetate reacts at room temperature with neat secondary amines at solvent-free conditions to form respective amides [44,45]. The general procedure involves mixing neat piperidine or morpholine with NC-$CH_2$-C(O)$OC_2H_5$ at 1.5 : 1 ratio under stirring and an $N_2$ blanket. These reactions within 24 – 60 hours at room temperature lead to prePiPCO (**1**) and preMCO (**4**) in high yields (Scheme 1). Course of both reactions was monitored by TLC watching disappearance of the cyanoacetylacetate. Since starting compounds and final cyan-acetamides do not contain chromophores, an $I_2$-chamber was used for plates' development. Thus, thick off-white precipitates of **1** and **4** were filtered under vacuum, washed with small portions (~20 mL) of toluene and hexane (~25 mL), and then dried in a *vacuum dessicator* charged with *concentrated $H_2SO_4$* for several days until smell of the amine was no longer detectable. Data for **1**: yield 92%, m.p. 87-90°C. The ring methylene protons in both precursors and target cyanoximes demonstrate complex non-first order $^1$H NMR spectra of *AA'BB'* spin systems. The $^1$H NMR, ppm, in dmso-$d_6$: 4.01 (singlet, 2H), ring protons - 3.41 ("triplet", 2H), 3.28 ("tiplet", 2H), 1.53 (multiplet, 6H). Mass-spectrometry, positive FAB (Ar): for $C_8H_{12}N_2O$, calculated - 152.12 (found - 152.1). Data for **4**: yield ~100%, m.p. 78-81°C, $R_f$ = 0.12 in EtOAc/hexane (1:2) mobile phase. The $^1$H NMR, ppm, in dmso-$d_6$: 4.03 (singet, 2H), ring protons - 3.56 ("quartet", 4H – next to O), 3.43 ("triplet", next to N), 3.34 ("triplet", next to N). Mass-spectrometry, positive FAB (Ar): for $C_7H_{10}N_2O_2$, calculated - 154.07 (found - 154.08).

***Synthesis of cyanoximes HPiPCO* (2) *and HMCO* (5)—**The general procedure includes the room temperature nitrosation reaction of precursors **1** and **4** with gaseous methylnitrite, $CH_3ONO$, at basic conditions according to published procedures [25c, 46] (Scheme 1; *ESI 1*).

Details of the syntheses are the following: for the HPiPCO, **2** – 60 mL of 1-propanol in a round-bottom flask in which 0.40 g (17.4 mM) of thinly sliced metallic sodium was dissolved. Both solutions were combined only before gaseous $CH_3ONO$ was allowed to pass through the mixture in order to avoid Thorpe condensation reactions encountered in the past. These occur between deprotonated substituted acetonitriles at basic conditions [47]. In a

NIH-PA Author Manuscript

NIH-PA Author Manuscript

NIH-PA Author Manuscript

separate Erlenmeyer flask 2.646 g (17.4 mM) of **1** were dissolved in ~100 mL of 1-propanol under stirring.

For the HMCO, **5** – 70 mL of 1-propanol in which 0.45 g (19.6 mM) of thinly sliced metallic sodium were dissolved; 3.016 g (19.6 mM) of **4** were dissolved in 80 mL of *n*propanol under intense stirring, and both solutions were combined immediately before $CH_3ONO$ introduction. The methylnitrite generator (which consisted of a three-necked 2 L flask with a 1:1 (by volume) mixture of methanol in water that contained 22 g of $NaNO_2$, and an addition funnel with cold, ~0°C, dilute 1:5 $H_2SO_4$ (*ESI 1*) was connected via glass pipe and a small piece of Tygon© tube, to the two flasks with basic solutions of **1** and **4** as outlined above. A flow of gaseous $CH_3ONO$ started with the slow addition of sulfuric acid to the methanol-water-sodium nitrite mixture. The gas allowed passing through mixtures of **1** and **4** within ~20 min. The color of these mixtures immediately changed to a bright-yellow, and soon thick yellow precipitates of Na-salts of HPiPCO and HMCO formed. Both flasks were left in the refrigerator for ~10 hrs at +4°C, and then the solvent was removed under vacuum using the rotary evaporator, followed with drying on an oil pump at ~40°C for 1 hr. Dried yellow solid residues from both flasks was re-dissolved in 100 mL of distilled water in separate 250 mL beakers forming yellow solutions, which were then acidified to a pH~4 with dilute HCl (1:5) added dropwise under stirring. The HPiPCO (**2**) as off-white thick precipitate immediately formed in a beaker with nitrosated precursor **1**, was filtered, washed with water and then dried under vacuum in a dessicator. The cyanoxime HMCO, **5**, has better solubility in water and did not precipitate, and was extracted from the aqueous solution which, prior to this was saturated with solid NaCl, with three portions of diethyl ether (20 mL, 30 mL and 50 mL), which were combined and dried over $MgSO_4$. Ether was removed under vacuum resulting in an off-white solid of pure HMCO. The HPiPCO (**2**) was obtained at 76% yield, it melts at 159°C; $R_f$ = 0.55 in ethanol / $CHCl_3$ = 9:1 mobile phase. The $^1H$ NMR, ppm, dmso-$d_6$: 14.31 (OH), ring protons - 3.54 ($CH_2$ *ortho*- to N), 2.50 ($CH_2$ *meta*- to N), 1.57 ($CH_2$, *para*- to N). Analysis for **2**, $C_8H_{11}N_3O_2$, calculated (found), %: C – 53.03 (53.10); H – 6.12 (6.07); N – 23.19 (22.96). Bands in the IR spectrum of **2**, $cm^{-1}$ (KBr): 3420, 2940, 2890, 2240, 1630, 1042. The HMCO (**5**) was obtained at ~60 % yield, it has m.p. 155°C; $R_f$ = 0.44 in EtOAc / hexane = 2:1 mobile phase. The $^1H$ NMR, ppm, dmso$d_6$: 14.29 (OH), ring protons - 3.30 ($CH_2$ next to O), 2.50 ($CH_2$ next to N). Analysis for **5,** $C_7H_9N_3O_3$, calculated (found), %: C – 45.90 (45.78); H – 4.95 (5.09); N – 22.94 (22.84). Bands in the IR spectrum of **5**, $cm^{-1}$ (KBr): 3430, 2977, 2834, 2235, 1627, 1010. Both cyanoximes are well soluble in ether, alcohols, acetone, acetonitrile, DMF, SMSO, pyridine (with color change to yellow due to deprotonation), but are insoluble in hydrocarbons and $CCl_4$.

***Synthesis of AgPiPCO* (3) *and AgMCO* (6)—**A high yield preparation of these silver(I) cyanoximates was accomplished in two steps as shown in Scheme 2. At first, the deprotonation of cyanoximes takes place in an aqueous solution with the addition of an equivalent amount of solid $K_2CO_3$, followed by the dropwise addition of an aqueous solution of $AgNO_3$ under intensive stirring. Thick yellow precipitates of AgL immediately form, were filtered using an M-grade glass filter, washed with water, and then dried in a vacuum dessicator charged with concentrated $H_2SO_4$. The yield for **3** was 89%, and the analysis for $AgC_8H_{10}N_3O_2$, calculated (found), %: C – 33.36 (33.39), H – 3.50 (3.37), N – 14.59 (14.36). The yield for **6** was 83%, and the analysis for $AgC_7H_8N_3O_3$, calculated (found), %: C – 28.99 (28.92), H – 2.78 (2.63), N – 14.49 (14.25). Both complexes are not soluble in water, acetone, hydrocarbons and halohydrocarbons, but exhibit moderate solubility in acetonitrile, nitromethane and are well soluble in DMF, DMSO and pyridine.

NIH-PA Author Manuscript

NIH-PA Author Manuscript

NIH-PA Author Manuscript

**Safety note:** the precursor **1** for the HPiPCO cyanoxime **2** is a mild lachrymator, and work with this waxy, low melting point substance should be carried out under the ventilation hood.

**Photophysical studies—**First, two sample holders were prepared from four strips of black cardboard, tape, and computer paper. Next, the Ag(I) salt was compressed into a uniform thickness on each sample holder (*ESI 2*). The samples rested in a wooden apparatus that held them in place. The UV light was laid directly on top of the wooden holder, approximately 2 cm away from the samples (*ESI 3*). The samples were exposed to thirty minutes of 254 nm light emitted from the low-pressure germicidal Hg-lamp. Previous measurements of intensity of this lamp using the UVX-radiometer (UK) provided values of energy delivered to the sample's surface as 13.1 J/cm$^2$ [34,56]. After each round of thirty minutes, the samples were removed from the UV light, photographed, and then underwent spectral analysis. The percent reflectance was measured in the 300-825 nm range for samples of **3** and **6** using the Varian Cary-100 Bio UV-Vis spectrophotometer equipped with the integrating sphere device DRA CA 301 (*ESI 3*), in which pure MgO was used as a standard (*ESI 28*).

## Acrylate polymeric composites containing AgL

For antimicrobial studies we prepared a light-curable flowable mixture that is commonly used in dental practice from commercial ingredients depicted in *ESI 4*. Silver(I) cyanoximates **3** and **6** were added to the mixture and thoroughly homogenized, and the resulting composite was added into a 96-wells plate via syringe as shown in *ESI 5*. Addition of silver(I) complexes took place on the balance pan, and all added amounts of compounds were expressed in weigh % due to convenience. It was found to be difficult to reproduce and make exactly same volume of the mixture in repeated experiments, but was much easier to add/adjust the amount of AgL to match desired mass concentrations that were arbitrary chosen for antimicrobial studies to be 0.5, 1, 2,5 and 5%. The mixture then was polymerized with the help of the Spectrum Curing Light source (λ~400 nm) used in dentistry (*ESI 6*), checked for solidness with a needle, and subjected to antimicrobial studies according to developed protocol.

## Microbiological studies: planktonic and biofilm growth assessment

The AgPIPCO (**3**) and AgMCO (**6**) compounds (0.5, 1, 2.5, and 5 %) were mixed into the dental polymeric composite material, and applied onto the surface of the wells in 96-well plates (Corning Inc., New York, USA). *Pseudomonas aeruginosa* strain PAO1, *Streptococcus mutans* strain UA159, and *Staphylococcus aureus* strain ST228 were used. Biofilms were quantitatively assayed using a quantitative 96-well microplate Crystal Violet assay as described previously [48]. Prior to plate inoculation, the cultures were grown in a 50% Brain Heart Infusion (BHI) medium to the middle log phase (determined based on the individual growth curves), collected, and diluted to obtain absorbance at 600 nm of 0.1. Dilutions 1:100 of thus standardized cultures were inoculated into fresh 50% BHI (for PAO1), 100% Tryptic soy broth (TSB) with 1% glucose at 5% $CO_2$ (for NRS70), or 100% BHI with 1% glucose (for UA159) and incubated for 24 h at 37°C. To measure planktonic growth, the cultures were transferred onto fresh plates, and the absorbance at 600 nm was measured using a Bio-tek Synergy HT microtiter plate reader (Tecan Instruments Inc.). The remaining biofilms were washed three times with 0.8 % NaCl to remove loosely attached cells and were stained with crystal violet (0.4%, w/v) for 10 min as described in [49]. The dye was solubilized in 33% (v/v) acetic acid, and the absorbance of the extracted stain was measured at 595 nm. Non-inoculated wells were measured as blanks and the corresponding measurements were subtracted from the rest of the data. Cells growing in the wells containing composites alone were used as positive controls. The data represent the mean

NIH-PA Author Manuscript

NIH-PA Author Manuscript

NIH-PA Author Manuscript

values of seven technical replicates and two biological replicates and are shown in Figures 8 and 9. Actual photographs of the 96-well plates before and after microbiological studies are shown in *ESI 7*.

## Results and Discussion

### Organic compounds

Both synthesized cyanoximes represent weak organic acids that demonstrate a single ionization process in solutions with pKa values of 5.31± 0.006 for **5**, 5.43±0.01 for **2** respectively. It should be noted that the ionization constants for other oximes is ~9.5 for the acetone-monoxime and $pK_1$ = 10.2 for the famous dimethylglyoxime [50], which reflects a very dramatic increase in several orders of magnitude of acidity of the cyanoximes due to the electron-withdrawing effect of the CN-group. Two cyanoximes selected for this study have markedly different hydrophobicity, with HMCO being the most hydrophilic due to the presence of the morpholyl-group as compared to the piperidine group for **2**.

**Crystal structures of cyanoximes and their precursors—**Solid state structures of substituted cyanacetamides **1** and **4** (precursors for target cyanoximes) were determined and presented in *ESI 8,9,12,13*. Crystal and refinement data for cyanoximes **2** and **5** are presented in Table 1, while selected bond lengths and valence angles for both cyanoximes are shown in Table 2. Molecular structures and numbering schemes for **2** and **5** are displayed in Figure 1. Details of crystal packing of both cyanoxime ligands can be found in the *ESI 14,15*. The structure of HPiPCO (**2**) contains two co-crystallized diastereomers of this cyanoxime – *syn* and *anti* (Figure 1). It should be noted, however, that this is not the case of the two-positional disorder, since upon dissolution in organic solvents there are two different isomers at room temperature that have different chemical shifts in the $^{13}C\{^1H\}$ NMR spectra. This is a fairly rare phenomenon for oximes since both geometrical isomers tend to crystallize separately [51,52]. Nevertheless, cocrystallization of two diastereomers was recently observed for several other mono- and bis-cyanoximes [44,53].

The aliphatic cyclic groups attached to the amide fragment in **2** and **5** adopt a chair conformation. There are two planar fragments in the core of both ligands. The value of the dihedral angle between cyanoxime and amide groups is 29.09º for **5** (*ESI 16*). Because of the presence of two diastereomers (*syn* and *anti*) the same values for **2** are 59.36º and 40.28º respectively (*ESI 17*). One of the most interesting features in the structures of both cyanoximes is a practically planar amide group: the values of dihedral angles between O2-C3-C1 and C7-N3-C4 mean planes are 8.03º for **5** and 5.29º for similar planes (for *syn*) and 16.31º (for *anti*) isomers of **2** (*ESI 17,18*). Packing of both cyanoximes in crystal is achieved via the formation of medium strength H-bonds between the oxygen atoms of the amide and oxime groups as shown in *ESI 14,15,19*. A very similar geometry of H-bonding in both diastereomers of **2** explains their cocrystallization in one unit cell. Crystal packing of both compounds can be described as regular, H-bonded chains that run along an a-direction (*ESI 14,15*). The achiral cyanoxime **5** crystallizes in a chiral $P2_12_12_1$ space group (Table 1) due to a specific screw-like H-bonding pattern that has handiness. Despite the low Flack parameter, it is not possible to determine the absolute configuration of HMCO (**5**), due to the absence of heavy atoms in the structure and the Mo-Kα radiation used for the structure determination.

**Spectroscopic studies—**The $^{13}C\{^1H\}$ NMR spectra of cyanoximes precursors – acetamides **1** and **4** – display all non-equivalent carbon atoms in rings due to a rotational barrier around C3-N2 amide bonds (*ESI 10,11*). Cyanoximes were found to be prone to form both *syn* and *anti* geometrical isomers as depicted in Figure 2. Contrary to traditional

NIH-PA Author Manuscript

NIH-PA Author Manuscript

NIH-PA Author Manuscript

organic olefins with >C=C< bonds with well-defined and thermally stable Z and E geometrical isomers, >C=N- double bond in some organic compounds is known to undergo thermal re-isomerization of geometrical isomers. This property was reflected in special terms (*syn* and *anti*) that were introduced to reveal the frequently observed interconversion of compounds containing an azomethine bond [54]. There are numerous cases of preparation of single-isomer oximes – either *anti* [51], or *syn* [29] – structures of which were confirmed by X-ray analysis. Nevertheless, as stated above, cyanoximes are often obtained as the mixture of both isomers at different ratios as evidenced from their $^{13}C\{^{1}H\}$ NMR spectra containing a double set of signals [44,46,52]. The HPiPCO (**2**) reported herein was obtained as a mixture of two isomers (*ESI 20,26,27*), while HMCO (**5**) appears as only one geometrical isomer (presumably *anti*) according to the $^{13}C$ NMR data (*ESI 21,25*).

Both studied cyanoximes **2** and **5** undergo deprotonation in solutions upon the addition of a base, which results in the formation of colored anions and the bathochromic shift and an intensity change in their UV-visible spectra (*ESI 22*). These anions possess pronounced negative solvatochromic behavior of their $n\ \pi^*$ transitions in spectra, which was reflected in a rather dramatic color change from pale-yellow in water to red-pink in DMSO (Figure 3; *ESI 22,23*). Thus, the energy difference between those transitions in water (380 nm; 26316 $cm^{-1}$) and DMSO (465 nm; 21506 $cm^{-1}$) for the anion $\mathbf{5}^-$ corresponds to 57.5 kJ/M (which is 20.13 kCal/M; 4810 $cm^{-1}$) strong H-bonding energy. Analogous data for the $\mathbf{2}^-$ anion yield are $\Delta\lambda$ = 87 nm (4998 $cm^{-1}$), or 59.8 kJ/M (20.91 kCal/M). These gaps in energy values for both cyanoximate anions in their solvatochromic series are significant and represent the highest known up-to-date among compounds with $n\rightarrow\pi^*$ transitions in UV-visible spectra. Also, very weak ($\varepsilon < 10$) $n\rightarrow\pi^*$ transitions [55] are also observable in spectra of alkaline metals salts above 900 nm in aqueous solutions (*ESI 22*). These can be associated with the formation of $Na(HL_2)$ salts of H-bridged bis-cyanoxime monoanion similar to the $Kat^+(HL_2)^-$ systems ($Kat^+ = Li^+, Na^+, K^+$; L = amide-cyanoxime NC-C(NO)-C(O)$NH^-_2$ [56,63]) and other systems that we observed in the past [64].

## Silver(I) complexes

Unfortunately, despite numerous attempts using several techniques (vapor diffusion, slow interlayer solvent diffusion, slow evaporation, etc.) we were not able to grow suitable for the X-ray analysis crystals of Ag(PipCO), **3**, and Ag(MCO), **6**. By their appearance and solubility pattern most likely both synthesized complexes represent coordination polymers similar to those we reported earlier [34-36]. This is also evident from similar IR-spectroscopic signatures of complexes **3** and **6** as compared to other silver(I) cyanoximates. Thus, characteristic shifts of $\nu$(C=O) and $\nu$(CNO), $\nu$(NO) bands indicate involvement of the nitroso-groups in bridging binding between the two silver(I) centers [29,47]. Both complexes **3** and **6** with time completely dissolve in DMSO and Py with the formation of 1:1 type electrolyte with the loss of original coordination-polymeric structure. UV-visible spectra of such solutions are not different from spectra of ionic alkali-metals salts.

**Photophysical Studies—**These investigations are important in view of using high-intensity light (UV and visible) to cure an acryl-amide based polymer composite for the intended application as an adhesive to be used to fix in place indwelling medical devices. The protocol for such work was developed in our previous studies of other silver(I) cyanoximates [56,57] and allows a direct comparison of their light stability. Reflectance spectra of studied compounds were recorded using MgO as a standard (*ESI 27*). Solid samples of AgL (compounds **3** and **6**) were prepared as shown and described in *ESI 3*. An intense white visible light and monochromated LED generated light ($\lambda$~400 nm) from a commercial dental curing device (*ESI 7*) do not cause the samples to darken.

NIH-PA Author Manuscript

NIH-PA Author Manuscript

NIH-PA Author Manuscript

Microscopic photographs of both samples which are remarkably stable to visible light are shown in Figure 4. However, UV-light from a low-pressure Hg-lamp slowly induces a change in the samples. Thus, samples of **3** and **6** were exposed to UV-light in 30 minutes increments for three hours until no further changes were observed. Contrary to conventional inorganic AgCl and $AgNO_3$ (*ESI 29*,*30*), studied silver(I) cyanoximates **3** and **6** did not turn black. Their reflectance spectra and actual samples' photographs are presented in Figures 5 and 6 respectively. Using the time profile of the reflectance change, graphs of the samples darkening were generated and allowed quantitative assessment of Ag(PiPCO), **3**, and Ag(MCO), **6**, stability towards UV-light. Thus, Figure 7 contains experimental data and their best fit as mono-exponential decay function upon samples darkening. The initial rate of complexes **3** and **6** degradation, therefore, could be calculated as *d(% reflectance)/d(time)* = -A/t, and compared with those obtained earlier for other silver(I) cyanoximates. Based on our observations, the most stable is the Ag(PiPCO) complex **3** with the initial rate of photodecomposition equal to -0.17±0.02 %/min, followed by the complex **6** with its much faster rate of decomposition equal to -0.47±0.03 %/min. It should be noted that the typical curing time (with ~400 nm light source) for dental acrylamide-based composites is 2-3 minutes, and both our compounds are perfectly stable towards UV-light at this time interval.

It was interesting and important to determine the cause of darkening of the studied complexes **3** and **6**. Our investigations of the origin of image darkening revealed that it is fine particles (nanometer size) of metallic silver, which is one of the products of the photoreduction of Ag(I) cyanoximates after more than three hours of the **3** and **6** solid samples' exposure to UV-radiation. Elemental silver forms colloid solutions in DMF, pyridine and DMSO, which exhibit the Tindal effect clearly. Silver particles also tend to aggregate in these solutions with time. However, further investigations of the dynamics of the particles' growth, and their shapes, sizes and weighted distribution were out of the scope of the first stage of this work, but certainly will be addressed in the future.

**Fabrication of polymer composites for microbiological studies:** Both synthesized and studied silver cyanoximates **3** and **6** demonstrated a very good miscibility and tolerance with the flowable polymeric matrix (*ESI 5*,*6*). This is an important finding in light of the intended practical applications for these complexes. After filling them with composite, all containing a different weight % of silver(I) cyanoximates and control lines, 96 wells plates were irradiated with visible light to cure the composite until it became solid (*ESI 31*). These plates were sterilized with UV-light (λ=254 nm) for 5 minutes to prevent contamination from air-born microorganisms and were then subjected to the microbiological studies described below.

**Microbiological studies:** To assess the effect of the silver(I) cyanoximates complexes on pathogenic bacteria, we characterized both planktonic and biofilm growth in the presence of these compounds. For this, the compounds were embedded into the polymeric composite, commonly used in dental practice, and applied onto the surface of the wells in 96-well plates. Three human pathogens, *P. aeruginosa* PAO1 (wound isolate) [58,59], *S. aureus* NRS70 (methicillin resistant respiratory isolate) [60], and *S. mutans* UA159 (cariogenic dental isolate) [61], causing biofilm-associated infections with different modes of pathogenicity, were selected. The data shown in the figures below represent the mean values of seven technical replicates and two biological replicates with the standard deviation plotted as error bars. Thus, planktonic measurements (Figure 8) showed that both compounds completely abolished the growth of PAO1 at 0.5 weight % concentration, and the growth of UA159 and NRS70 at 1% concentration. Biofilm measurements (Figure 9) showed a higher resistance of the tested bacteria to the compounds. This was expected, since biofilms, in general are known for their elevated resistance to antimicrobials [62]. The

NIH-PA Author Manuscript

NIH-PA Author Manuscript

NIH-PA Author Manuscript

presence of Ag(MCO) in the composite completely inhibited the biofilm formation in PAO1 and UA159 at 1 %, whereas NRS70 showed a greater ability to produce a biofilm and was inhibited by 98 % at a 5 weight % of Ag(MCO). Similarly, the presence of Ag(PiPCO) completely abolished the ability of PAO1 to produce a biofilm at 1 %, however, it showed a much stronger effect on NRS70, inhibiting its growth at 2.5%. The biofilm growth of UA159 was inhibited by 92 % at a 2.5 weight % of Ag(PiPCO).

Overall, the data demonstrate that Ag(MCO), **6**, and Ag(PiPCO), **3**, inhibit both planktonic and biofilm growth of Gram-positive and Gram-negative bacterial pathogens where the latter complex performs slightly better. Therefore, studied silver(I) cyanoximates have a strong potential in antimicrobial applications as effective additives to acrylate-based light-curable polymeric composites that are used as adhesives during fixing indwelling medical devices.

## Conclusions

1. A high-yield synthesis of desired cyanoximes (**2**, **5**) and their precursors (**1**, **4**) was developed using two stage preparations of compounds from cyanoacetic acid esters and cyclic secondary amines such as piperideine and morpholine, and then the nitrosation reaction with gaseous $CH_3ONO$ afforded target cyanoximes. Synthesized cyanoximes were investigated by means of IR, $^{1}H$, $^{13}C$ and UV-visible spectroscopy. Crystal structures of 4 compounds (2 precursors and 2 cyanoximes) were determined.

2. Two silver(I) complexes of AgL composition (L = PipCO, **3**; MCO, **6**) were prepared in high yield and characterized by elemental analysis and IR spectroscopy. Both complexes are thermally stable up to ~135°C, and totally stable to high intensity visible light. Both complexes demonstrate a slow, within ~3 hrs, photoreduction observable as a gradual color change and darkening due to the formation of fine (nano-scale) particles of metallic silver. The complex Ag(MCO), **6**, is about 2.6 times less stable towards UV-radiation than its more lypophyllic analog Ag(PipCO), **3**.

3. Both silver(I) cyanoximates showed a very good tolerance and miscibility with the flowable acrylate-based light-curable composites commonly used in dental practice. A remarkable stability of silver(I) cyanoximates **3** and **6** towards visible light is a very important property for photo-induced cross-linking fabrication of polymers. Several solid, light-cured polymeric composites containing different mass percent (0.5, 1, 2,5 and 5%) of dispersed in the polymer complexes **3** and **6** were fabricated. Curing was done using a commercial dental light source.

4. Antimicrobial and biofilm growth inhibition properties of prepared solid polymeric composites containing silver(I) cyanoximates were investigated on three human pathogens such as: *P. aeruginosa* PAO1 (wound isolate), *S. aureus* NRS70 (methicillin resistant respiratory isolate), and *S. mutans* UA159 (cariogenic dental isolate). Studies showed that both **3** and **6** compounds completely abolished the growth of PAO1 at a 0.5 weight % concentration, and the growth of UA159 and NRS70 at a 1% concentration. Moreover, the data demonstrates that complexes **3** and **6** also inhibit both planktonic and biofilm growth of Gram-positive and Gram-negative bacterial pathogens with the former complex performing slightly better. Therefore, both silver(I) cyanoximates demonstrated the strong potential for the studied complexes to be used as light insensitive antimicrobial additives to adhesives that set indwelling devices in place.

NIH-PA Author Manuscript

NIH-PA Author Manuscript

NIH-PA Author Manuscript

## Supplementary Material

Refer to Web version on PubMed Central for supplementary material.

## Acknowledgments

Authors thank NIH for financial support of this investigation from an award 1R15AI088594-01A1. NG is grateful to the MSU Department of Chemistry and the Graduate College for help at the beginning of this project. NG is thankful to Ms. Alexandra Corbett for technical help during the manuscript preparation.

## References

1. Romling U, Balsalobre C. Journal of internal medicine. 2012; 272:541. 2012. [PubMed: 23025745]
2. Alipour M, Suntres ZE, Omri A. The Journal of antimicrobial chemotherapy. 2009; 64:317. [PubMed: 19465435]
3. Hentzer M, Givskov M. The Journal of clinical investigation. 2003; 112:1300. [PubMed: 14597754]
4. Lynch AS, Robertson GT. Annual review of medicine. 2008; 59:415.
5. Nicolas GG, Lavoie MC. Can. J. Microbiol. 2011; 57:1. [PubMed: 21217792]
6. National Science Foundation Press Release. 2011:11–230.
7. a Klasen HJ. Burns. 2000; 26:131. [PubMed: 10716355] b Rujitanaroj P, Pimpha N, Supaphol P. Polymer. 2008; 49(11):4723.c Valappil SP, Pickup DM, Carroll DL, Hope CK, Pratten J, Newport RJ, Smith ME, Wilson M, Knowles JC. Antimicr. Agents and Chemotherapy. 2007; 51(12):4453.d Feng QL, Wu J, Chen GQ, Cui FZ, Kim TN, Kim JO. Journal of biomedical materials research. 2000; 52:662. [PubMed: 11033548]
8. Kawashita MS, Tsuneyama F, Miyaji T, Kokubo H, Kozuka H, Yamamoto K. Biomaterials. 2000; 21:393–398. [PubMed: 10656321]
9. Alt V, Bechert T, Steinrucke P, Wagener M, Seidel P, Dingeldein E, Domann E, Schnettler R. Biomaterials. 2004; 25:4383. [PubMed: 15046929]
10. Toshikazu T. Inorganic Mater. 1999; 6:505.
11. Rujitanaroj P, Pimpha N, Supaphol P. Polymers. 2008; 49(11):4723.
12. Santoro CM, Ducsherer NL, Grainger DW. Nanobiotechnology. 2007; 3(2):55. [PubMed: 19865601]
13. Valappil SP, Pickup DM, Carroll DL, Hope CK, Pratten J, Newport RJ, Smith ME, Wilson M, Knowles JC. Antimicr. Agents and Chemotherapy. 2007; 51(12):4453.
14. a Lippard, SJ., editor. Platinum, Gold, and Other Metal Chemotherapeutic Agents: Chemistry and Biochemistry. American Chemical Society; Washington DC: 1983. b Blower PB. Inorganic pharmaceuticals; Annual Reports in Progress in Chemistry. 2001; 97:587–603. Sect. A. c Cotton, AF.; Wilkinson, G.; Murillo, CA.; Bohmann, M. Advanced inorganic chemistry. 6th ed.. John Wiley & Sons; New York: 1999.
15. a Chugaev LA. Chem. Ber. 1905; 38:2520.b Chugaev LA. J. Chem. Soc. London. 1914; 125:2187.
16. Samus NM, Ablov AV. Coord. Chem. Rev. 1979; 28:177.
17. Milios SJ, Samatatos TC, Perlepes SP. Polyhedron. 2006; 25(1):134.
18. Pavlischuk V, Birkelbach F, Weyhermuller T, Wieghardt K, Choudhuri P. Inorg. Chem. 2002; 41(17):4405. [PubMed: 12184757]
19. a Bagai R, Abboud KA, Christou G. Inorg. Chem. 2007; 46(14):5567. [PubMed: 17547392] b Zaleski CM, Weng T-C, Dendrinou-Samara C, Alexiou M, Kanakaraki P, Hsien W-Y, Kampf J, Penner-Hann JE, Pecoraro VL, Kessisoglou DP. Inorg. Chem. 2008; 47(14):6127. [PubMed: 18537236] c Zhang S, Zhen L, Xu B, Inglis R, Li K, Chen W, Zhang Y, Konidaris KF, Perlepes SP, Brechin EK, Li Y. Dalton Trans. 2010; 39:3563. [PubMed: 20354610]
20. Stamatatos TC, Diamantopolou E, Raptopolou CP, Psycharis V, Esner A, Perlepes SP. Inorganic Chemistry. 2007; 46(7):2350. [PubMed: 17328543]
21. Baffert C, Artero V, Fontecave M. Inorganic Chemistry. 2007; 46(5):1817. [PubMed: 17269760]

NIH-PA Author Manuscript

NIH-PA Author Manuscript

NIH-PA Author Manuscript


22. Follert AD, McNabb KA, Peterson AA, Scanlon JD, Cramer CJ, McNeill K. Inorganic Chemistry. 2007; 46(5):1645. [PubMed: 17286398]
23. Ram MS, Riordan CG, Yap GPA, Liable-Sands L, Rheinhold AL, Marchaj A, Norton JR. J. Am. Chem. Soc. 1997; 119(7):1648.
24. a Palii, GK.; Skopenko, VV.; Gerasimchuk, NN.; Makats, EF.; Domashevskaya, OA.; Rakovskaya, RV. 1988. Patent of the USSR, #1405282b Skopenko, VV.; Palii, GK.; Gerasimchuk, NN.; Domashevskaya, OA.; Makats, EF. 1989. Patent of the USSR, #1487422c Skopenko, VV.; Palii, GK.; Gerasimchuk, NN.; Makats, EF.; Domashevskaya, OA.; Rakovskaya, RV. 1988. Patent of the USSR #1405281d Ciba Geigy AG. Patent of Poland. 127786:1985.e Davidson, SH. 1978. Patent of the USA #3957847f Ciba Geigy, AG. 1982. Patent of Austria # 367268
25. a Gerasimchuk N, Maher T, Durham P, Domasevitch K, Wilking J, Mokhir A. Inorganic Chemistry. 2007; 46(18):7268. [PubMed: 17676728] b Eddings D, Barnes C, Durham P, Gerasimchuk NN, Domasevich KV. Inorganic Chemistry. 2004; 43(13):3894–3909. [PubMed: 15206870] c Charlier, H.; Gerasimchuk, N. 2010. Patent of the USA N$^{o}$ 7,727,967 B2
26. Gerasimchuk NN, Simonov, Yu. A, Dvorkin AA, Rebrova ON. Russ. J. Inorg. Chem. 1993; 38(2): 247.
27. Mokhir AA, Gerasimchuk NN, Pol'shin EV, Domasevitch KV. Russ. J. Inorg. Chem. 1994; 39(2): 289.
28. Kogan VA, Burlov AS, Popov LD, Lukov VV, Yu. V, Koschienko EB, Tsupak GP, Barchan GG, Chigarenko VS. Bolotnikov. Koord. Khim. 1987; 13(7):879.
29. Gerasimchuk N, Goeden L, Durham P, Barnes CL, Cannon JF, Silchenko S, Hidalgo I. Inorg. Chim. Acta. 2008; 361:1983.
30. Maher, Tiffany. MS Thesis: “Synthesis, Characterization and Anti-cancer properties of Organotin(IV) Cyanoximates,”. Southwest Missouri State University, Department of Chemistry; Springfield, USA: 2004. p. 123
31. Eddings, Daniel. MS Thesis: “The Synthesis, Characterization, Spectroscopic, and Biological Activity Studies of Pt(II) and Pd(II) Cyanoximates,”. Southwest Missouri State University, Department of Chemistry; Springfield, USA: 2003. p. 154
32. Gerasimchuk, N.; Glover, G. “Visible light insensitive silver(I) cyanoximates.” Inorganic chemistry section, poster presentation (196).. 237 Spring National ACS Meeting; Salt Lake City, UT. March 22-26th, 2009;
33. Gerasimchuk, N. New Trends in Coordination, Bioinorganic, and Applied Inorganic Chemistry. Melník, M.; Seg'a, P.; Tatarko, M., editors. Slovak University of Technology Press; 2011. p. 106-113.ISBN 978-80-227-3509-4
34. Glower G, Gerasimchuk N, Biagioni R, Domasevitch K. Inorg. Chem. 2009; 48(6):2371. [PubMed: 19267497]
35. Gerasimchuk N, Esaulenko AN, Dalley KN, Moore C. Dalton Transactions. 2010; 39:749. [PubMed: 20066220]
36. Gerasimchuk N, Gamian A, Glover G, Szponar B. Inorganic Chemistry. 2010; 49(21):9863. [PubMed: 20873734]
37. Fromm, KM.; Brunetto, P.; Vig Slenters, T. ”Nanostructured implant surface coating with antimicrobial properties” Abstracts of Papers. 237th ACS National Meeting; Salt Lake City, UT, USA. March 22-26th, 2009; COLL-347
38. Slenters TV, Hauser-Gerspach I, Daniels AU, Fromm KM. J. Mater. Chem. 2008; 18(44):5359.
39. Kasuga NC, Sato M, Amano A, Hara A, Tsuruta S, Sugie A, Nomiya K. Inorg. Chim. Acta. 2008; 361(5):1267.
40. Software Package for Crystal Structure Solution, APEX 2. Bruker AXS; Madison, WI: 2009.
41. a Blessing RH. Acta Crystallogr. 1995; A51:33.b Sheldrick, GM. SADABS Area-detector Absorption Correction, 2.03. University of Göttingen; Göttingen, Germany: 1999.
42. a Farrugia L. J. Appl. Crystallogr. 1997; 30:565.b Burnett, MN.; Johnson, CK. ORTEP III: Report ORNL-6895. Oak Ridge National Laboratory; Oak Ridge, TN: 1996.
43. CCDC crystallographic viewing and graphing software package Mercury 4.2.

NIH-PA Author Manuscript

NIH-PA Author Manuscript

NIH-PA Author Manuscript


44. The list of all 37 cyanoximes can be found in ESI for the paper Cheadle, C.; Gerasimchuk N, Barnes CL, Tyukhtenko SI, Silchenko S. Dalton Transactions. 2013; 42(14):4931. [PubMed: 23385567] Research groups working with cyanoximes: Australia (S. Batten), Canada (S. Bohle), Ukraine (K. Domasevitch, R. Lampeka, V. Pavlischuk, S. Kolodilo, I. Fritskiy, T. Sliva), Poland (H. Kozlowski, E. Gumiena-Kontezka), South Africa (I. Nikolaenko), Spain (A. Escuer), Greece (S. Perlepes), USA (N. Gerasimchuk).
45. Domasevitch KV, Skopenko VV, Gerasimchuk NN. Doklady Akademii Nauk Ukrainskoi RSR. 1989; 5(B):26.
46. Curtis S, Ilkun O, Brown A, Silchenko S, Gerasimchuk N. Cryst. Eng. Comm. 2013; 15:152.
47. Goeden, Leon. MS Thesis “The Synthesis, Characterization and Bilogical Activity Studies of Pt(II) and Pd(II) Disubstituted Arylcyanoximates,”. Southwest Missouri State University, Department of Chemistry; Springfield, USA: 2005. p. 182
48. Ahmed SA, Gogal RM, Walsh JE. J. Immunol. Meth. 1994; 170:211.
49. O'Toole GA, Kolter R. Molecular microbiology. 1998; 28:449–61. [PubMed: 9632250]
50. a CRC Handbook of Chemistry and Physics. 56th Ed.. CRC Press; Chemical Rubber Co; 1974. b Dean, JA. Lange's Handbook of Chemistry. 14th Ed.. McGraw-Hill; New York: 1992.
51. Chertanova L, Paskard C, Sheremetev A. Acta Cryst. 1994; B50:708. (and references therein).
52. Mokhir AA, Domasevich KV, Kent Dalley N, Xiaolan Kou NN, Gerasimchuk OA. Gerasimchuk. Inorg. Chim. Acta. 1999; 284:85.
53. Robertson D, Cannon J, Gerasimchuk N. Inorganic Chemistry. 2005; 44(23):8326. [PubMed: 16270971]
54. Eliel, E.; Wielen, S. Stereochemistry of Organic Compounds. Wiley Interscience; 1994. p. 1267
55. Feuer, H.; Krieger, R., editors. The Chemistry of the Nitro- and Nitroso- Groups. Publishing Co.; Huntington, NY, USA: 1981. part 1
56. Morton, Jeff. MS Thesis “Further Investigations of Silver(I) Cyanoximates,”. Missouri State University, Department of Chemistry; USA: 2010. p. 138
57. Whited, M.; Morton, J.; Gerasimchuk, N. “Investigations of stability of polyacrylamide composites containing antimicrobial silver(I) cyanoximates to high intensity visible and UV-light.” Abstracts of Papers. 243rd ACS National Meeting; San Diego, CA, USA. March 25-29, 2012; INOR-314Morton, JR.; Gerasimchuk, N. “Silver(I) Cyanoximates: Synthesis, Crystal Structures and Physical Properties.”. Presentation at the 239th National American Chemical Society Meeting; San Francisco, CA, USA. March 21-25th 2010; INOR-947
58. Stover CK, Pham XQ, Erwin, et al. Nature. 2000; 406:959–964. [PubMed: 10984043]
59. Ohman DE, Chakrabarty AM. Infect Immun. 1981; 33:142. [PubMed: 6790439]
60. Kuroda M, et al. The Lancet. 2001; 357:1225.
61. Ajdic D, McShan WM, McLaughlin RE. Genome sequence of Streptococcus mutans UA159, a cariogenic dental pathogen. PNAS. 2002; 99:14434. [PubMed: 12397186]
62. Høiby N, Bjarnsholt T, Givskov M, Molin S, Ciofu O. Int. J. Antimicrob. Agents. 2010; 35(4):322. 2010. [PubMed: 20149602]
63. Domashevskaya OA, Mazus MD, Dvorkin AA, Simonov, Yu. A, Gerasimchuk NN. Russ. J. Inorganic Chemistry. 1988; 33(12):3026.
64. Domasevich KV, Gerasimchuk NN, Rusanov EB, Gerasimchuk OA. Russ. J. Gen. Chem. 1996; 66(4):635.

NIH-PA Author Manuscript

NIH-PA Author Manuscript

NIH-PA Author Manuscript

## HIGHLIGHTS

- Two new cyanoxime ligands and their precursors were synthesized
- Compounds were characterized using NMR, UV-visible spectra, X-ray analysis.
- Two new light-stable silver(I) cyanoximates were obtained and characterized.
- Acrylate-based polymeric composites containing Ag(I) cyanoximates were prepared
- Antimicrobial activity and biofilm inhibition of two silver(I) complexes was established

NIH-PA Author Manuscript

NIH-PA Author Manuscript

NIH-PA Author Manuscript

## SYNOPSIS

Two silver(I) complexes of AgL composition (L = new cyanoxime ligands PipCO, **3**; MCO, **6**) were prepared in high yield and characterized by elemental analysis and IR spectroscopy. Both complexes are thermally stable, and totally stable to high intensity visible light. Silver(I) cyanoximates showed a very good tolerance and miscibility with the flowable acrylate-based light-curable composites commonly used in dental practice. Several solid, light-cured polymeric composites containing different mass percent (0.5, 1, 2,5 and 5%) of dispersed in the polymer complexes **3** and **6** were fabricated. Antimicrobial and biofilm growth inhibition properties of prepared solid polymeric composites containing silver(I) cyanoximates were investigated on three human pathogens such as: *P. aeruginosa* PAO1 (wound isolate), *S. aureus* NRS70 (methicillin resistant respiratory isolate), and *S. mutans* UA159 (cariogenic dental isolate). Studies showed that both **3** and **6** compounds completely abolished the growth of PAO1 at a 0.5 weight % concentration, and the growth of UA159 and NRS70 at a 1% concentration. Moreover, the data demonstrates that complexes **3** and **6** also inhibit both planktonic and biofilm growth of Gram-positive and Gram-negative bacterial pathogens with the former complex performing slightly better.

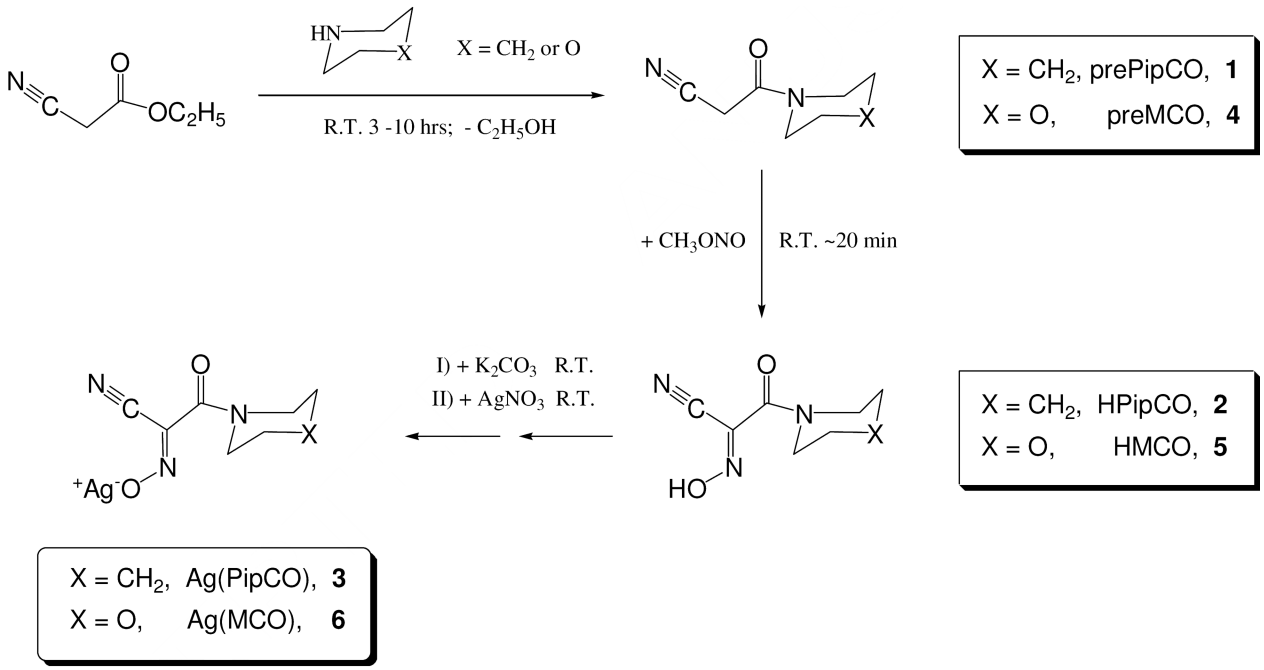


**Scheme 1.**
synthetic route to cyanoximes and their Ag-complexes



NIH-PA Author Manuscript NIH-PA Author Manuscript NIH-PA Author Manuscript

NIH-PA Author Manuscript
NIH-PA Author Manuscript
NIH-PA Author Manuscript



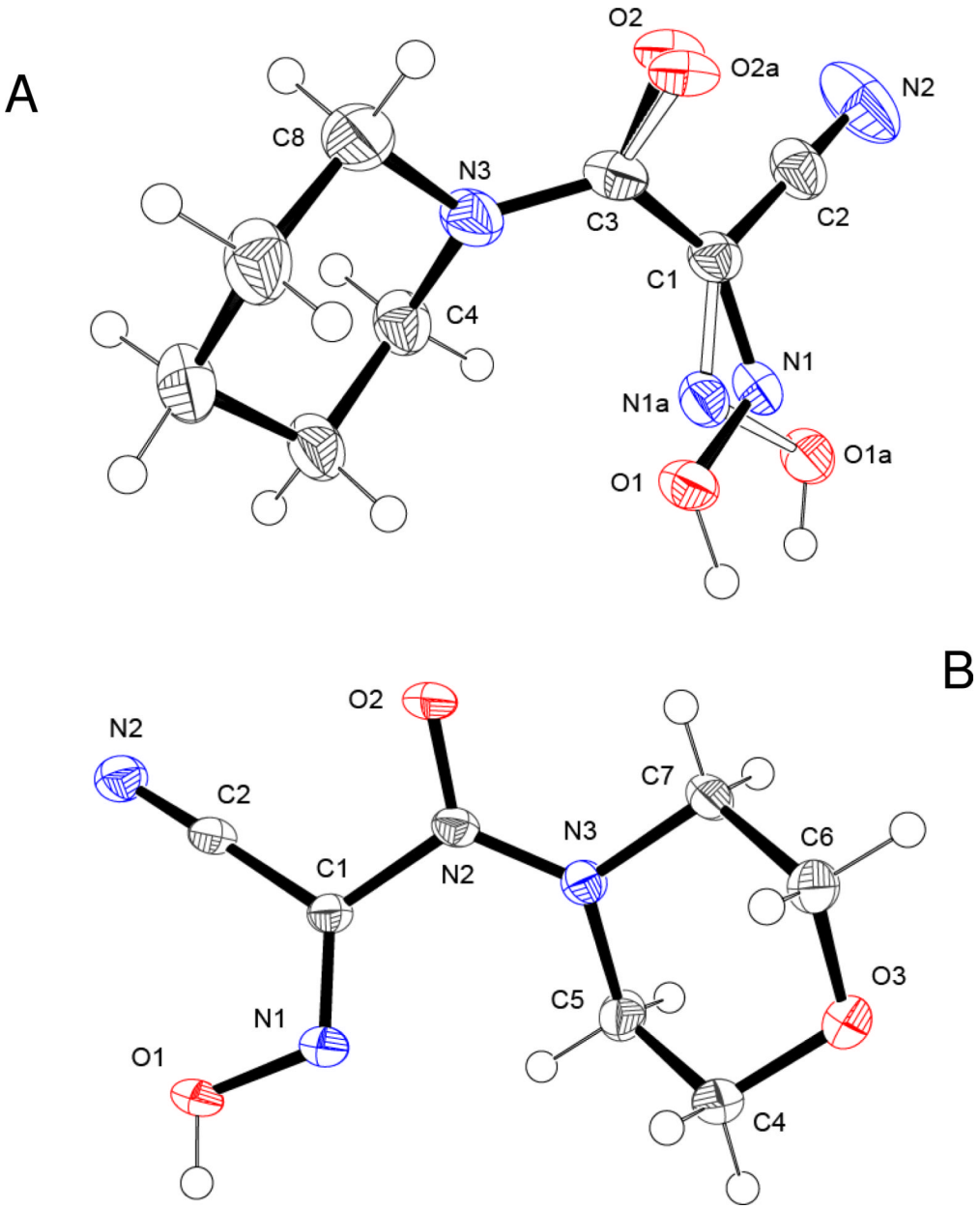


**Figure 1.**
Molecular structures and numbering schemes for HPiPCO (**A,** two diastereomers - syn and anti - are shown), and HMCO (**B**); an ORTEP drawing at 50% thermal ellipsoids probability.

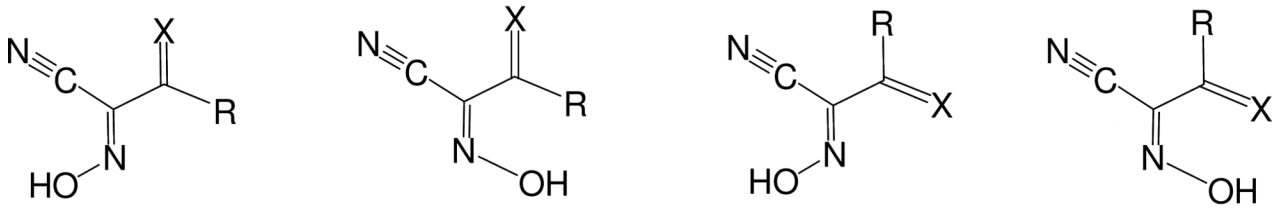


$X = O, S, Se; \quad R = NH_2, \ N(CH_3)_2, \ N(C_2H_5)_2, \ C(CH_3)_3, \ C_6H_5$

**Figure 2.**
Geometrical isomers observed in cyanoximes and their metal complexes.



NIH-PA Author Manuscript NIH-PA Author Manuscript NIH-PA Author Manuscript

NIH-PA Author Manuscript

NIH-PA Author Manuscript

NIH-PA Author Manuscript

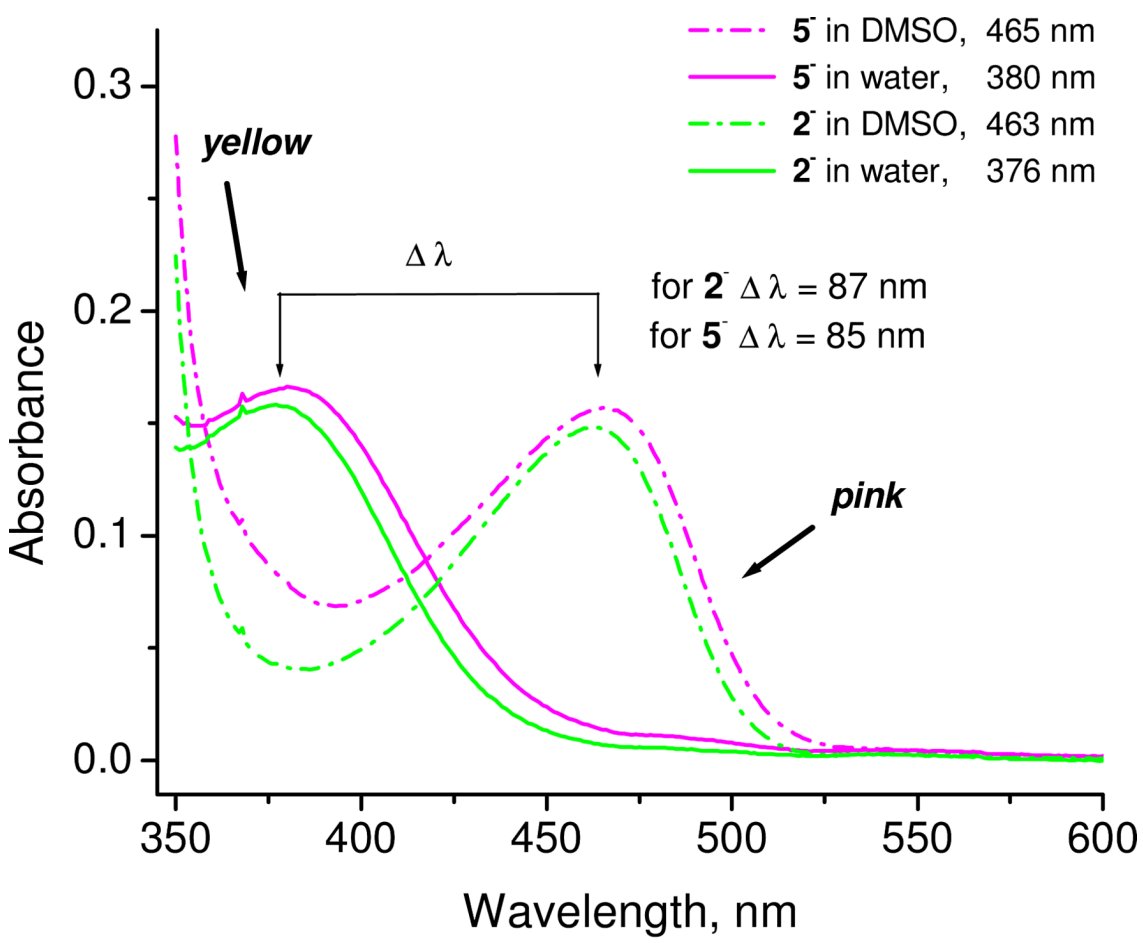


**Figure 3.**
Visible spectra of isomolar solutions (5 mM) of cyanoxime anions of $\mathbf{2}^-$ (green) and $\mathbf{5}^-$ (pink) in water, and DMSO. For recording these spectra initial cyanoximes were deprotonated with one drop of $N(C_4H_9)_4OH$ solution; 1 cm cuvette, T=296 K.

NIH-PA Author Manuscript

NIH-PA Author Manuscript

NIH-PA Author Manuscript

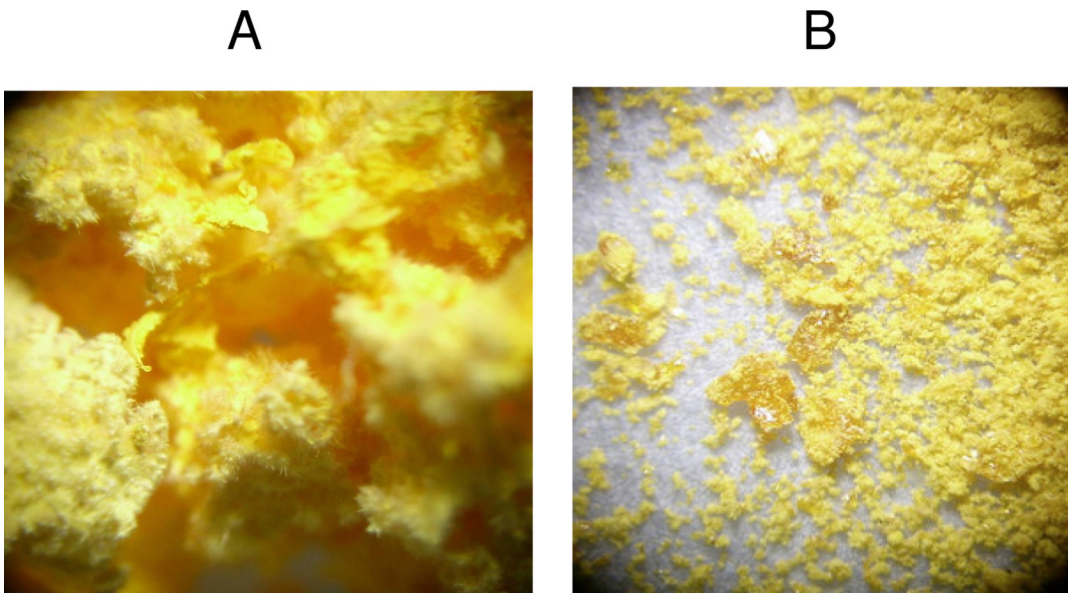


**Figure 4.**
Actual photographs of dry, powdery **6**, Ag(MCO) (**A**) and **3**, Ag(PiPCO) (**B**) under the microscope at 40x magnification.

NIH-PA Author Manuscript

NIH-PA Author Manuscript

NIH-PA Author Manuscript

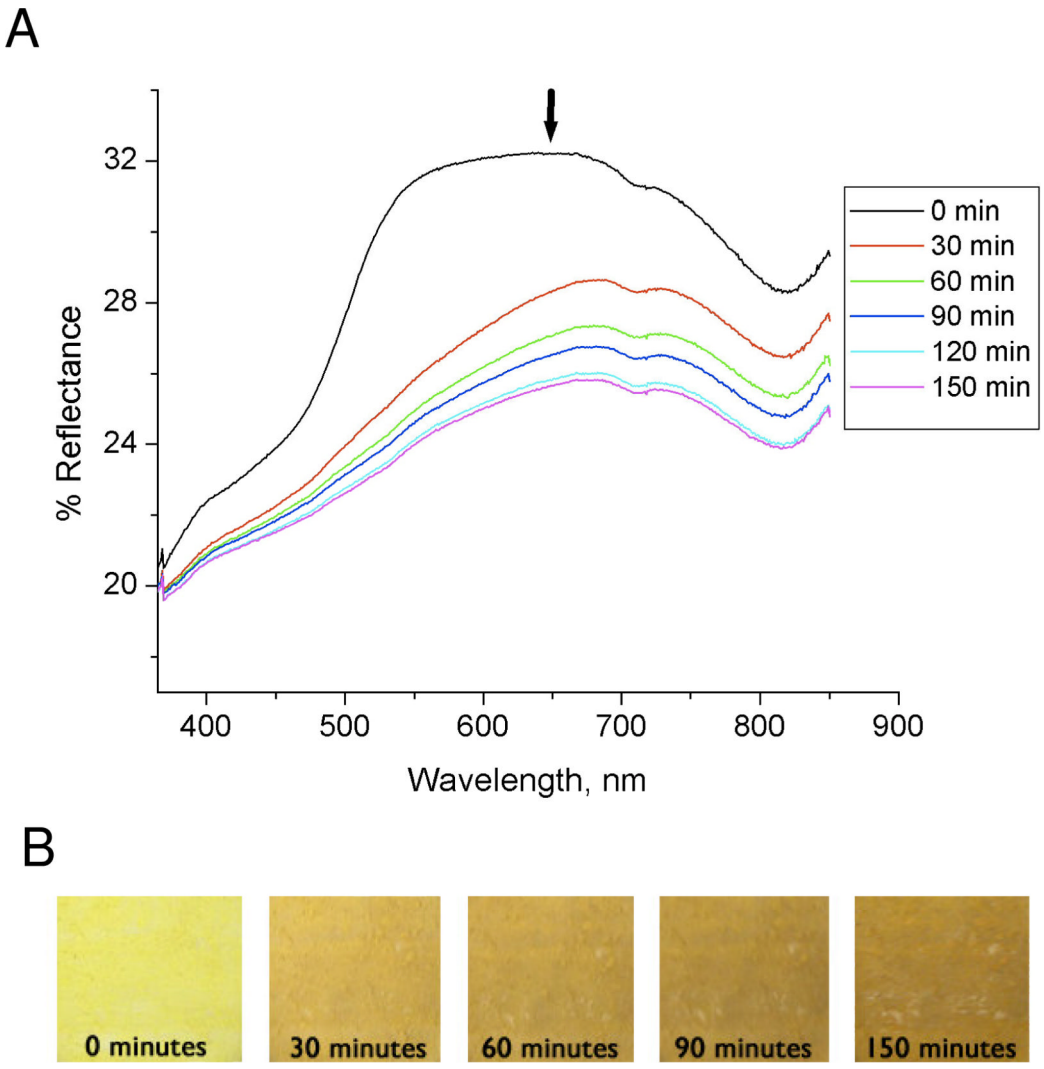


**Figure 5.**
Diffusion reflectance spectra changes for the sample of Ag(PiPCO), **3**, with time of exposure to UV-light (**A**); an arrow points on a significant samples reflectance decrease due to darkening. Actual photographs of samples over time (**B**).

NIH-PA Author Manuscript

NIH-PA Author Manuscript

NIH-PA Author Manuscript

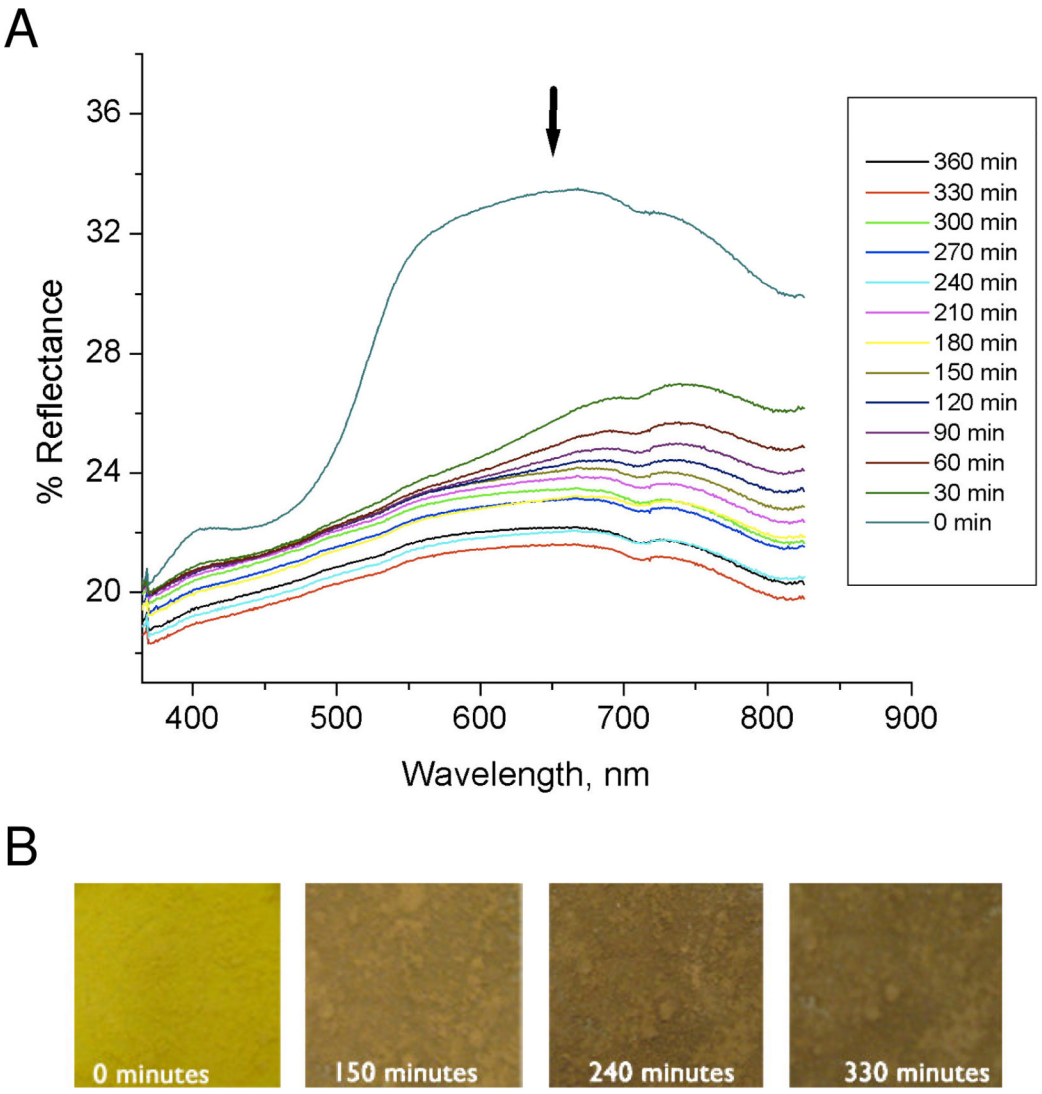


**Figure 6.**
Spectroscopic changes of the Ag(MCO), **6**, sample reflectance over time of exposure to UV-light (**A**); actual photographs of samples over time (**B**).

NIH-PA Author Manuscript
NIH-PA Author Manuscript
NIH-PA Author Manuscript



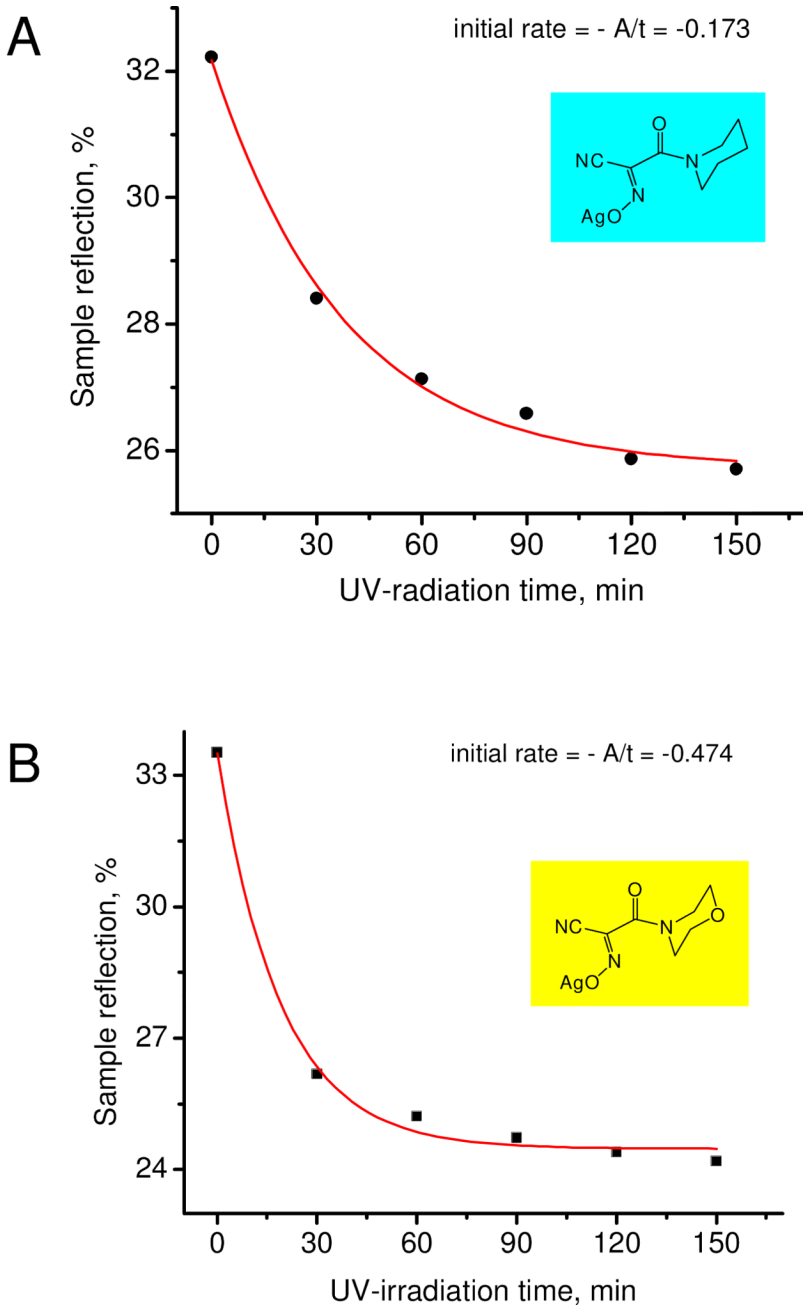


**Figure 7.**

Time dependence of AgL samples reflectance change upon irradiation with the UV-light source. **A** – Ag(PiPCO) with data fit the best to a monoexponential decay function $y = y_0 + A\, e^{(-x/t)}$ with the following parameters: $y_0 = 25.72 \pm 0.21$; $A = 6.45 \pm 0.29$; $t = 37.34 \pm 4.55$; $\chi^2 = 0.05669$ and $R^2 = 0.9943$. **B** – Ag(MCO), best fit to a monoexponential decay function $y = y_0 + A\, e^{(-x/t)}$ with the following parameters: $y_0 = 24.48 \pm 0.17$; $A = 9.02 \pm 0.34$; $t = 19.03 \pm 2.24$; $\chi^2 = 0.09001$ and $R^2 = 0.99577$.

NIH-PA Author Manuscript

NIH-PA Author Manuscript

NIH-PA Author Manuscript

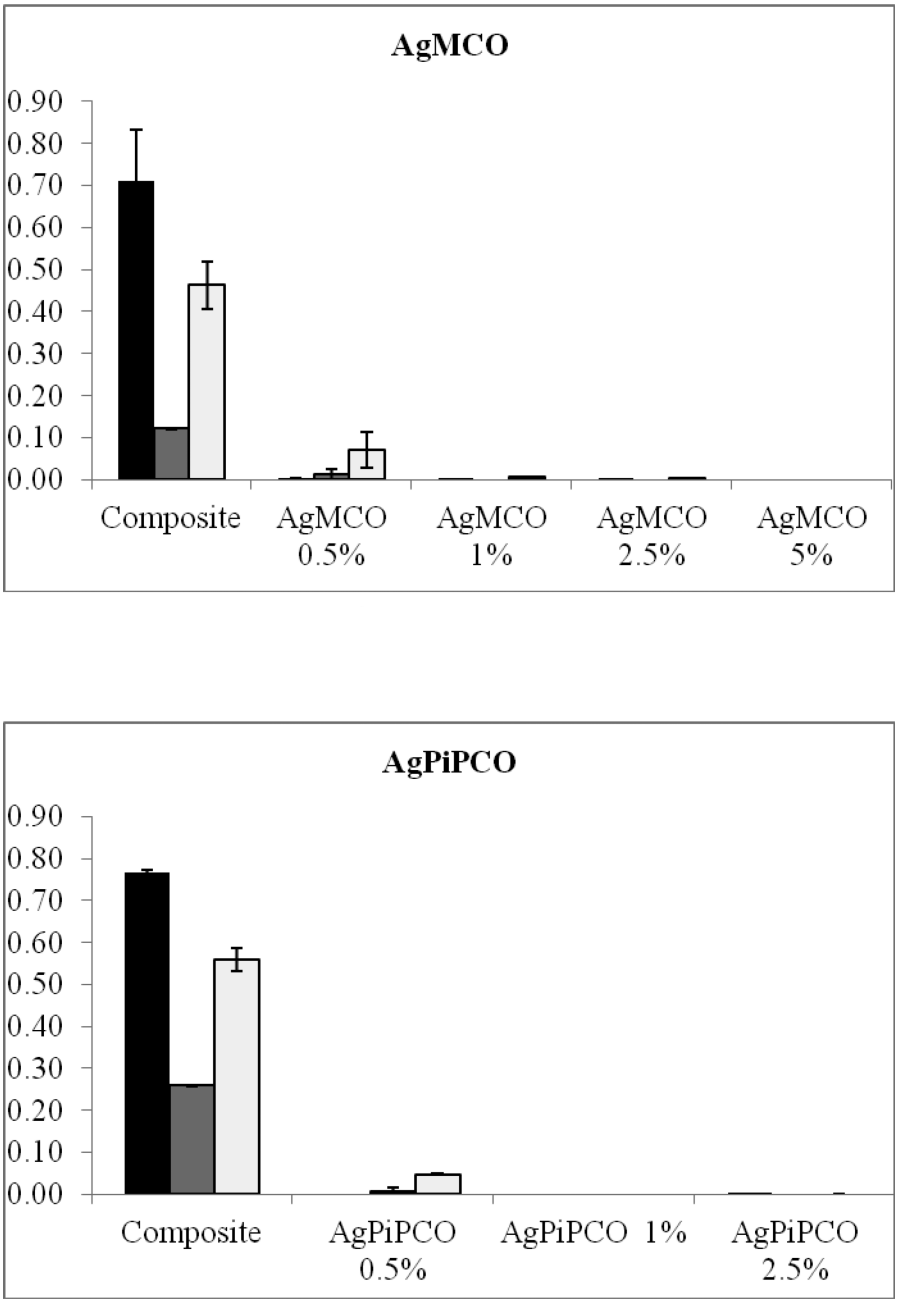


**Figure 8.**

Planktonic growth of *P. aeruginosa* PAO1 (black), *S. aureus* NRS70 (dark grey), and *S. mutans* UA159 (light grey) in the wells containing composites with embedded compounds: Upper – Ag(MCO), **6**, lower – Ag(PiPCO), **3**. The wells containing composites alone were used as positive controls.

NIH-PA Author Manuscript

NIH-PA Author Manuscript

NIH-PA Author Manuscript

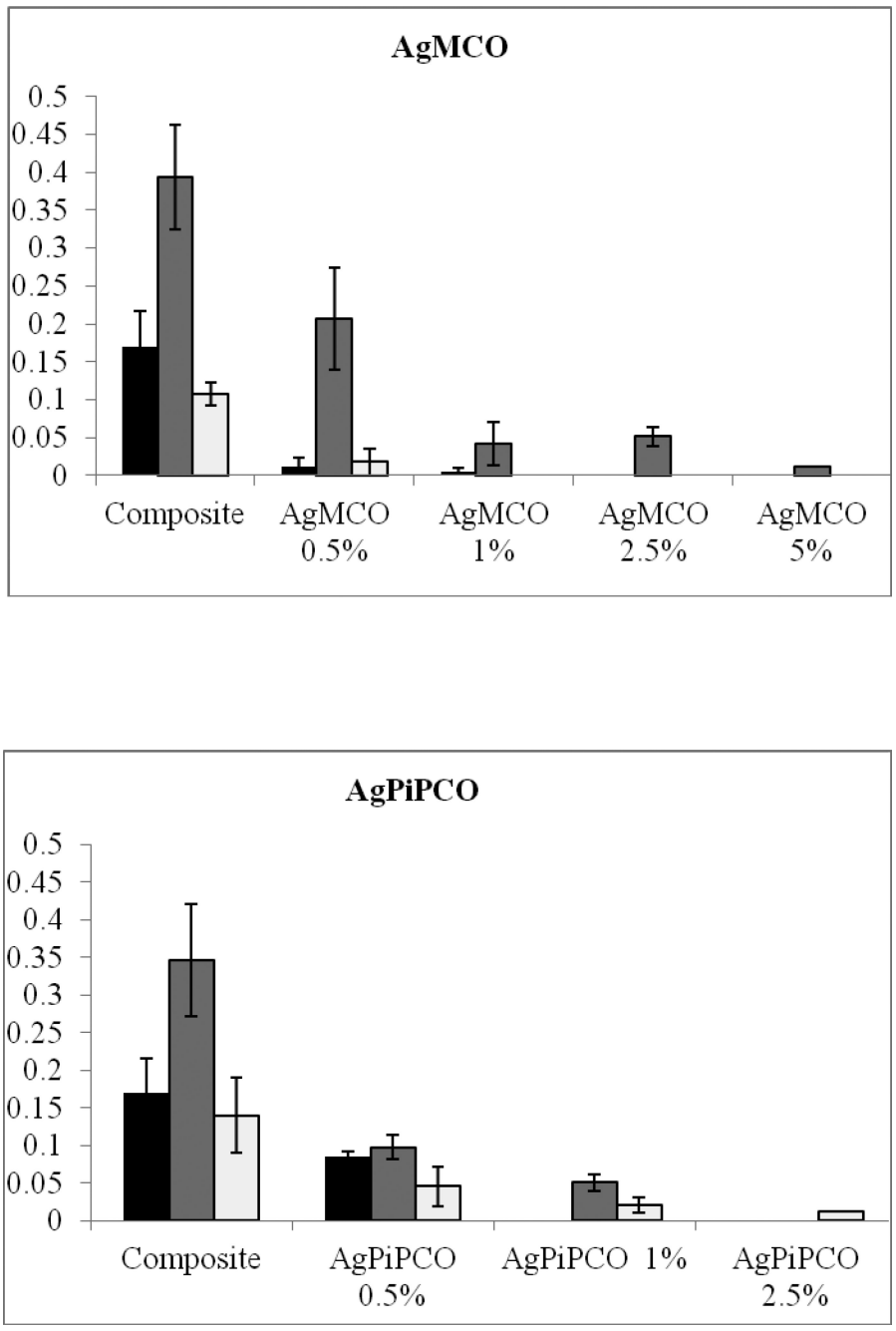


**Figure 9.**

Biofilm growth of *P. aeruginosa* PAO1 (black), *S. aureus* NRS70 (dark grey), and *S. mutans* UA159 (light grey) in the wells containing composites with embedded compounds: Upper – Ag(MCO), **6**, lower – Ag(PiPCO), **3**. The wells containing composites alone were used as positive controls.

NIH-PA Author Manuscript
NIH-PA Author Manuscript
NIH-PA Author Manuscript



**Table 1**

Crystal data and structure refinement for synthesized cyanoximes.

| | H(MCO), **5** | H(PiPCO), **2** |
|---|---|---|
| Empirical formula | $C_7 H_9 N_3 O_3$ | $C_8 H_{11} N_3 O_2$ |
| Formula weight | 181.20 | 183.17 |
| Temperature | 120(2) K | 120(2) K |
| Wavelength, Mo | 0.71073 Å | 0.71073 Å |
| Crystal system | Orthorhombic | Monoclinic |
| Space group | P $2_1$ $2_1$ $2_1$ | P $2_1$/c |
| Unit cell dimensions | a = 6.7259(4) Å | a = 6.3513(16) Å. |
| | b = 9.4836(6) Å | b = 13.942(4) Å |
| | c = 13.2127(9) Å | c = 10.580(3) Å |
| | α= 90° | α= 90° |
| | β= 90° | β= 95.003(3)° |
| | γ = 90° | γ = 90° |
| Volume | 842.78(9) $Å^3$ | 909.2(2) $Å^3$ |
| Z | 4 | 4 |
| Density (calculated), $Mg/m^3$ | 1.444 | 1.324 |
| Absorption coefficient, $mm^{-1}$ | 0.115 | 0.098 |
| F(000) | 384 | 384 |
| Crystal size, mm | 0.56 × 0.37 × 0.31 | 0.51 × 0.32 × 0.18 |
| Index ranges | −9<=h<=9 | −8<=h<=8 |
| | −12<=k<=12 | −19<=k<=19 |
| | −18<=l<=18 | −14<=l<=14 |
| Reflections collected | 10780 | 12040 |
| Independent reflections | 2200 [R(int) = 0.0275] | 2512 [R(int) = 0.0381] |
| Refinement method | Full-matrix least-squares on $F^2$ | |
| Data / restraints / parameters | 2200 / 0 / 118 | 2512 / 4 / 145 |
| Goodness-of-fit on $F^2$ | 1.052 | 1.039 |
| Final R indices [I>2σ (I)] | R1=0.0308, wR2=0.0761 | R =0.050, wR2=0.1062 |
| R indices (all data) | R1=0.0332, wR2=0.0782 | R1=0.071, wR2=0.1177 |
| Absolute structure parameter | −0.1(9) | n/a |
| Largest diff. peak and hole, e. $Å^{-3}$ | 0.262 and −0.195 | 0.323 and −0.367 |

NIH-PA Author Manuscript

NIH-PA Author Manuscript

NIH-PA Author Manuscript

## Table 2

Selected Bond lengths [Å] and angles [°] in structures of studied cyanoximes.

| **Bonds:** | | **Angles:** | |
|---|---|---|---|
| | | **HPiPCO, 2** | |
| C(1)-N(1) | 1.294(6) | N(1)-C(1)-C(2) | 108.2(3) |
| C(1)-N(1A) | 1.322(9) | N(1A)-C(1)-C(2) | 134.4(5) |
| C(1)-C(2) | 1.442(4) | N(1)-C(1)-C(3) | 135.2(3) |
| C(1)-C(3) | 1.511(4) | N(1A)-C(1)-C(3) | 109.45(19) |
| C(2)-N(2) | 1.147(4) | C(2)-C(1)-C(3) | 115.5(2) |
| C(3)-O(2) | 1.257(10) | N(2)-C(2)-C(1) | 179.5 (3) |
| C(3)-O(2A) | 1.255(18) | O(2A)-C(3)-N(3) | 123.3(17) |
| C(3)-N(3) | 1.324(4) | O(2)-C(3)-N(3) | 125.8(9) |
| C(4)-N(3) | 1.472(4) | O(2)-C(3)-C(1) | 114.2(8) |
| C(8)-N(3) | 1.476(4) | N(3)-C(3)-C(1) | 119.7(2) |
| N(1)-O(1) | 1.372(5) | C(3)-N(3)-C(8) | 120.1(3) |
| O(1)-H(1) | 0.98(7) | C(3)-N(3)-C(4) | 125.9(2) |
| N(1A)-O(1A) | 1.369(8) | C(8)-N(3)-C(4) | 114.0(2) |
| O(1A)-H(1A) | 0.8400 | C(1)-N(1)-O(1) | 110.1(4) |
| | | N(1)-O(1)-H(1) | 104(4) |
| | | N(1A)-O(1A)-H(1A) | 109.5 |
| | | C(1)-N(1A)-O(1A) | 107.2(8) |
| | | O(2A)-C(3)-C(1) | 116.3(17) |
| | | **HMCO, 5** | |
| C(1)-N(1) | 1.2819(14) | N(1)-C(1)-C(2) | 121.62(11) |
| C(1)-C(2) | 1.4508(16) | N(1)-C(1)-C(3) | 122.90(10) |
| C(1)-C(3) | 1.5026(16) | C(2)-C(1)-C(3) | 115.11(10) |
| C(2)-N(2) | 1.1414(16) | N(2)-C(2)-C(1) | 178.48(12) |
| C(3)-O(2) | 1.2382(14) | O(2)-C(3)-N(3) | 123.59(11) |
| C(3)-N(3) | 1.3305(15) | O(2)-C(3)-C(1) | 114.84(10) |
| C(4)-N(3) | 1.4681(15) | N(3)-C(3)-C(1) | 121.51(10) |
| C(7)-N(3) | 1.4703(14) | C(1)-N(1)-O(1) | 112.18(10) |
| N(1)-O(1) | 1.3723(13) | C(3)-N(3)-C(4) | 127.51(10) |
| O(1)-H(1) | 0.8400 | C(3)-N(3)-C(7) | 120.07(10) |
| | | C(4)-N(3)-C(7) | 112.17(9) |
| | | N(1)-O(1)-H(1) | 109.5 |